Title

Determination of a Comprehensive Alternative Splicing Regulatory Network and Combinatorial Regulation by Key Factors during the Epithelial-to-Mesenchymal Transition

Journal

Molecular and Cellular Biology, 36(11)

ISSN

0270-7306

Authors

Yang, Yueqin
Park, Juw Won
Bebee, Thomas W
et al.

Publication Date

2016-06-01

DOI

10.1128/mcb.00019-16

Peer reviewed

AMERICAN SOCIETY FOR MICROBIOLOGY | Molecular and Cellular Biology

Determination of a Comprehensive Alternative Splicing Regulatory Network and Combinatorial Regulation by Key Factors during the Epithelial-to-Mesenchymal Transition

Yueqin Yang,[a,b] Juw Won Park,[c,d,e] Thomas W. Bebee,[a,b] Claude C. Warzecha,[a,b]* Yang Guo,[c,f] Xuequn Shang,[f] Yi Xing,[c] Russ P. Carstens[a,b]

Departments of Genetics[a] and Medicine,[b] Perelman School of Medicine, University of Pennsylvania, Philadelphia, Pennsylvania, USA; Department of Microbiology, Immunology and Molecular Genetics, University of California, Los Angeles, Los Angeles, California, USA[c]; Department of Computer Engineering and Computer Science[d] and KBRIN Bioinformatics Core,[e] University of Louisville, Louisville, Kentucky, USA; School of Computer Science, Northwestern Polytechnical University, Xi'an, China[f]

The epithelial-to-mesenchymal transition (EMT) is an essential biological process during embryonic development that is also implicated in cancer metastasis. While the transcriptional regulation of EMT has been well studied, the role of alternative splicing (AS) regulation in EMT remains relatively uncharacterized. We previously showed that the epithelial cell-type-specific proteins epithelial splicing regulatory proteins 1 (ESRP1) and ESRP2 are important for the regulation of many AS events that are altered during EMT. However, the contributions of the ESRPs and other splicing regulators to the AS regulatory network in EMT require further investigation. Here, we used a robust *in vitro* EMT model to comprehensively characterize splicing switches during EMT in a temporal manner. These investigations revealed that the ESRPs are the major regulators of some but not all AS events during EMT. We determined that the splicing factor RBM47 is downregulated during EMT and also regulates numerous transcripts that switch splicing during EMT. We also determined that Quaking (QKI) broadly promotes mesenchymal splicing patterns. Our study highlights the broad role of posttranscriptional regulation during the EMT and the important role of combinatorial regulation by different splicing factors to fine tune gene expression programs during these physiological and developmental transitions.

Alternative splicing (AS) is a process by which a single gene transcript can be differentially spliced to yield numerous splice variants that can encode different protein isoforms and thereby greatly expand the protein coding capacity of the genome. Nearly all human genes are alternatively spliced, and cell-type-specific protein isoforms have been shown to be functionally essential for cell fate and viability (1–3). This process is under complex regulation by various *cis* elements in pre-mRNAs and their cognate binding partners, mainly RNA-binding proteins (RBPs). Splicing-regulatory RBPs recruited to their respective binding sites can have positive or negative effects on the splicing of different exons or splice sites. Many RBPs with largely ubiquitous expression in different tissues and cells have been shown to have broad impacts on splicing and important cell functions, such as SR and hnRNP protein families (4). However, several tissue-specific RBPs, such as NOVA, PTBP2 (nPTB), MBNL, and RBFOX proteins, have recently been described as having important roles as essential regulators of tissue- or cell-type-specific splicing (5–9). In order to further define a "splicing code" that controls broad patterns of tissue-specific splicing, as well as those that occur during developmental transitions, it is essential to characterize in greater detail how these tissue-specific regulators fine-tune AS programs combinatorially with more ubiquitously expressed splicing regulators (10).

The epithelial-to-mesenchymal transition (EMT) is a process by which epithelial cells transdifferentiate into mesenchymal cells, which involves extensive changes at the cellular and molecular levels. The epithelial cells lose apical-basolateral polarity through disruption of polarity complexes, which requires disassembly of cell junctions, including tight junctions (TJs), adherens junctions (AJs), desmosomes, and gap junctions, and become motile and invasive through cytoskeletal reorganization (11). This process, however, is reversible and, together with the reverse process, mesenchymal-to-epithelial transition (MET), plays a fundamental role in embryogenesis and organogenesis (12, 13). Furthermore, EMT has also been implicated in cancer metastasis, as well as the generation of cancer stem cells (CSCs) or tumor initiating cells (TICs) that are predictive of a poor response to cancer therapies (14–16). Most previous studies of the molecular mechanisms underlying EMT have mainly focused on signaling pathways and transcriptional regulation. In response to external growth factors or other cues, signaling pathways like transforming growth factor β (TGF-β) induce the expression of mesenchymal transcription

Received 8 January 2016 **Returned for modification** 19 February 2016
Accepted 28 March 2016

Accepted manuscript posted online 4 April 2016

Citation Yang Y, Park JW, Bebee TW, Warzecha CC, Guo Y, Shang X, Xing Y, Carstens RP. 2016. Determination of a comprehensive alternative splicing regulatory network and combinatorial regulation by key factors during the epithelial-to-mesenchymal transition. Mol Cell Biol 36:1704–1719. doi:10.1128/MCB.00019-16.

Address correspondence to Yi Xing, yxing@ucla.edu, or Russ P. Carstens, russcars@upenn.edu.

* Present address: Claude C. Warzecha, Eunice Kennedy Shriver National Institute of Child Health and Human Development, National Institutes of Health, Bethesda, Maryland, USA.

Y.Y. and J.W.P. contributed equally to this work.

Supplemental material for this article may be found at http://dx.doi.org/10.1128/MCB.00019-16.

factors, such as SNAIL, ZEB1/2, and TWIST, which in turn promote EMT through repression of epithelial genes and activation of mesenchymal genes. A hallmark of EMT is downregulation of the epithelial protein CDH1 (E-cadherin), which promotes disassembly of AJs. In addition, mesenchymal proteins, such as CDH2 (N-cadherin) and VIM (vimentin), are also well-described standard molecular markers that are upregulated during EMT. Previous studies established that TGF-β, as well as the mesenchymal transcription factors Snail1 and Zeb1, induces a robust and rapid EMT and characterized global changes in total gene expression, including those of standard EMT markers (17, 18).

Until recently, the role of posttranscriptional gene regulation in EMT has been relatively unexplored. We previously identified the epithelial splicing regulatory proteins 1 and 2 (ESRP1 and ESRP2) as cell-type-specific regulators of an epithelial cell-specific splicing program that is reverted during EMT (19, 20). We showed that *ESRP1* is transcriptionally inactivated during EMT, and studies by other groups have also confirmed that *ESRP1* is among the most downregulated genes in multiple EMT model systems (17–19, 21–24). Conversely, RBFOX2 generally promotes mesenchymal splicing patterns for many gene transcripts that undergo AS during EMT, although in some cases it promotes epithelial splicing (24–27). Moreover, it was shown that depletion of RBFOX2 impaired the invasiveness of cells that underwent EMT (21, 24). Interestingly, we showed that for some EMT-associated AS events, there is a combinatorial regulation between the ESRPs and RBFOX2 (27). In addition to the ESRPs and RBFOX2, several other RBPs, such as PTBP1 and MNBL, have also been implicated in AS regulation during EMT, although their functions are less well defined (21, 25). Additionally, the role of posttranscriptional regulation in EMT has also been shown to involve important epithelial cell-specific microRNAs that target *ZEB1*, and downregulation of these microRNAs is similarly observed during EMT (28, 29).

To date, there has been only one published study that investigated genomewide alterations in AS that accompany EMT using RNA-Seq (21). While this important study identified large-scale alterations in AS, many regulated events likely eluded detection due to the limited sequencing depth by current standards and the absence of biological replicates. In addition, the combinatorial regulation of AS by different splicing regulators at distinct time points during EMT is still poorly resolved, and contributions by novel EMT regulatory proteins remain to be uncovered. To more comprehensively determine the AS network during EMT, we used a robust inducible *in vitro* EMT model with high sequencing depth and multiple replicates to conduct an in-depth investigation of AS, including a temporal analysis at multiple time points during EMT induction. Although we previously determined genomewide AS targets of the ESRPs, the degree to which loss of ESRP expression contributes to splicing switches during EMT has not been characterized. We therefore carried out a parallel RNA-Seq analysis of ESRP targets in the same cell line and determined not only that the ESRPs are major regulators for AS during EMT but also that other splicing factors contribute to EMT-associated AS switches. For example, we defined novel roles for RBM47 and Quaking (QKI) in combinatorial regulation of AS during EMT. Together, these investigations help lay the groundwork for further studies to define the functional consequences of AS during EMT and how they affect this essential developmental process and relevant disease pathophysiology.

MATERIALS AND METHODS

Plasmids. pGIPZ-shESRP1 #3 and pGIBZ-shESRP2 #7, as well as the corresponding nontargeting control vectors, psPAX2 and pCMV-VSV-G, were described previously (19). We PCR amplified the cDNA sequence for the red fluorescent protein mCherry and used it to replace the coding sequence for enhanced green fluorescent protein (EGFP) in pGIBZ to derive pRIBZ-shESRP2 and the corresponding control vector pRIBZ-shCtrl (sequences and cloning strategies are available upon request). Note that these short hairpin RNA (shRNA) vectors facilitated visualization of transduction (green or red fluorescence) and drug selection (puromycin or blasticidin). The pGIPZ-shRBM47 expression vector was purchased from GE Dharmacon (V3LSH_393928). The pTet-On advanced vector was purchased from Clontech (catalog number 631069). We cloned the rtTA-Advanced cassette into the pIBX vector described previously using EcoRI and BamHI sites to make the pIBX-Tet-On vector (30). The pTRE-tight vector was purchased from Clontech (catalog number 631059). To enable selection, we cloned the TRE-CMVmin element into the pcDNA3 vector to derive pcDNA3-TRE-CMVmin. A subsequent construct, pcDNA-TRE-CMVmini-C-FF(B)-mCherry, was derived by inserting a sequence encoding a 2× FLAG tag followed by the coding sequence for mCherry. The coding sequence for *Zeb1* was subsequently inserted upstream from the sequences for the FLAG tag and mCherry to derive pcDNA3-TRE-CMVmin-C-FF(B)-mCherry-Zeb1, which encodes Zeb1 with C-terminal FLAG and mCherry (sequences and cloning strategies are available upon request).

Cell culture and transfection. Human non-small cell lung cancer cell line H358 (obtained from the American Type Culture Collection) and the H358 Zeb1 clone were maintained in RPMI 1640 with 10% fetal bovine serum (FBS) (catalog number SH30071.03; GE). 293T and MDA-MB-231 cells were maintained in Dulbecco modified Eagle medium (DMEM) with 10% FBS. To make a Tet-On-inducible Zeb1 H358 clone, H358 cells were first transfected with the pIBX-Tet-On plasmid using Lipofectamine 2000 (catalog number 11668027; Life Technologies) according to the manufacturers' protocols, selected in 10 μg/ml blasticidin for 2 weeks, and serially diluted in 96-well plates to obtain single-cell-derived clones. Second, pcDNA3-TRE-CMVmin-C-FF(B)-mCherry-Zeb1 was transfected into the H358 Tet-On clone using Lipofectamine 2000, selected in 500 μg/ml G418 (catalog number 10131035; Life Technologies), and serially diluted to derive single-cell clones. For the EMT time course experiment, the Tet-On–inducible Zeb1 H358 cells were seeded in 6-cm dishes in biological triplicate. Then, we treated the cells with 1 μg/ml doxycycline every other day for 7 days in total to induce and maintain Zeb1 expression. During the time course, we harvested RNA and protein each day for downstream analyses. Note that cells reached confluence at day 2 and day 4; therefore, we trypsinized and replated following the isolation of RNA at the day 2 and 4 time points.

Viral packaging and transduction. Lentiviral production and transduction were performed as described previously (19). Briefly, 293T cells were transfected in 6-cm dishes with 3 μg of the shRNA expression vector, 2.7 μg of psPAX2, and 300 ng of pCMV-VSV-G using TransIT-293 (product number MIR2700; Mirus). After 16 to 20 h, the medium was replaced with fresh DMEM with 10% FBS, and virus was harvested after an additional 24 h. Target cells were transduced with a 50/50 mixture of viral supernatant and growth medium. Selection was carried out using 2 μg/ml puromycin and/or 10 μg/ml blasticidin for 48 to 96 h. RNA and protein were harvested 7 to 8 days postinfection. ESRP and RBM47 knockdown using shRNAs, followed by RNA-Seq experiments, were both done in biological triplicates.

RNA interference using siRNA. Small interfering RNA (siRNA) for *RBM47* (target sequence CACGGTGGCTCCAAACGTTCA [catalog number SI04356884]) and *QKI* (no. 6, target sequence CCCGAAGCTGGTTTA ATCTAT [catalog number SI04218221], and no. 7, target sequence CAGAG TACGGAAAGACATGTA [catalog number SI04367342]) were purchased from Qiagen. siRNAs for *ESRP1* and *ESRP2* were previously described (30). The nonspecific Allstar siRNA (catalog number SI03650318) was pur-

chased from Qiagen as a negative control. Briefly, cells were seeded in 6-well plates and transfected with siRNAs twice over a period of 48 h using Lipofectamine RNAiMAX (catalog number 11778075; Life Technologies). A total of 30 pmol siRNA was used for each transfection. RNA was extracted 24 to 48 h after the second siRNA transfection (72 to 96 h following the first transfection). Knockdown of ESRP and/or RBM47 using siRNAs to test the combinatorial effect was done in biological triplicates. Knockdown of QKI in MDA-MB-231 cells was also done in biological triplicate.

RT-PCR and qRT-PCR. Total RNA was extracted using TRIzol (catalog number 15596018; Life Technologies). Reverse transcription (RT)-PCR was performed as described previously (30). The primers used for AS target validation, the exon sizes, and the PCR product sizes are summarized in Table S6 in the supplemental material. RT-quantitative PCR (qRT-PCR) analysis was performed and analyzed as described previously (30). 18S was used as an endogenous control for normalization. Each qRT-PCR represents average data from a technical triplicate. A one-tailed unpaired *t* test was used to calculate the *P* values for all RT-PCR and qRT-PCR results from biological triplicates. Graphs in the figures show the mean results ± standard deviations. TaqMan assay probes for human *ESRP1* (Hs00214472_m1), *ESRP2* (Hs00227840_m1), *RBM47* (Hs01001785_m1), *QKI* (Hs00287641_m1), and *18S* (Hs03003631_g1) were purchased from Life Technologies.

Antibodies and Western blotting. Total cell extracts were harvested in radioimmunoprecipitation assay (RIPA) buffer with protease inhibitor cocktail, phenylmethylsulfonyl fluoride (PMSF), and sodium orthovanadate (sc-24948; Santa Cruz). Immunoblotting was performed as described previously (30). Antibodies to the following proteins were used: ESRP1/2 (mouse, 1:200, 23A7) (19), RBM47 (rabbit, 1:1,000, SAB2104562; Sigma), QKI (rabbit, 1:200, HPA019123; Sigma), vimentin (mouse, 1:500, MS-129-P1; Thermo Scientific), CDH1 (24E10) (rabbit, 1:500, no. 3195; Cell Signaling), ZEB1 (rabbit, 1:1,000, sc-25388; Santa Cruz), FLAG (mouse, 1:5,000, F1804; Sigma), and β-actin (mouse, 1:5,000, A2228; Sigma). Secondary antibodies were purchased from GE Healthcare Life Sciences (sheep anti-mouse IgG NA931 and donkey anti-rabbit IgG NA934V, from 1:1,000 to 1:10,000).

cDNA libraries and RNA-Seq. One microgram total RNA was used to make each cDNA library, using the TruSeq stranded mRNA LT sample prep kit (catalog number RS-122-2102; Illumina) for the EMT time course and ESRP1/2 knockdown experiments and the NEBNext Ultra directional RNA library prep kit for Illumina (catalog number E7420S; NEB) for the RMB47 knockdown experiment. For cDNA library preparation using the NEB kit, poly(A) selection from total RNA was done using the NEBNext poly(A) mRNA magnetic isolation module (catalog number E7490S; NEB). One hundred-base-pair paired-end RNA-Seq using the Illumina Hiseq 2000 or Hiseq 2500 was done by Penn Genome Frontiers Institute (PGFI) or the Next-Generation Sequencing Core (NGSC) facilities at the University of Pennsylvania.

RNA-Seq analysis. We mapped RNA-Seq reads to the human genome (hg19) and transcriptome (Ensembl, release 72) using TopHat (version1.4.1), allowing up to 3 bp of mismatches per read and up to 2 bp of mismatches per 25-bp seed. We computed RNA-Seq-based gene expression levels (fragments per kilobase of exon per million fragments mapped [FPKM] metric) using Cuffdiff (version 2.2.0) and identified differential gene expression between the two sample groups at a false discovery rate (FDR) of <5%, >twofold difference in gene expression based on average FPKM, and minFPKM of >0.1 (31). We identified differential AS events between the two sample groups using rMATS version 3.0.8 (http://rnaseq-mats.sourceforge.net), which detects five major types of AS events from RNA-Seq data with replicates (32). In each rMATS run, the first group was compared to the second group to identify differentially spliced events with an associated change in the percent spliced in (ΔPSI or $\Delta\psi$) of these events. We ran rMATS using the −c 0.0001 parameter to compute *P* values and FDRs of splicing events with a cutoff $|\Delta\psi|$ of >0.01% and then collected the splicing events with an FDR of <5% and a $|\Delta\psi|$ of ≥5%.

Motif enrichment analysis. We performed motif enrichment analysis as described previously to identify binding sites of splicing factors and other RNA binding proteins (RBPs) that were significantly enriched in differential exon skipping events (33). We used 115 known binding sites (motifs) of RBPs from the literature (8, 27, 34–36), including well-known splicing factors. We examined the enrichment of the RBPs in the exon body and in 250 bp of upstream and downstream introns separately.

RNA map analysis. To identify the RNA binding map of the ESRPs for the differential skipped-exon (SE) events between two groups compared to those for control alternative exons, we examined ESRP binding sites using the top 12 GU-rich binding motifs previously identified by systematic evolution of ligands by exponential enrichment coupled with high-throughput sequencing (SELEX-Seq) (27). If an alternative exon didn't show splicing changes (rMATS FDR of >50%, maxPSI of >15%, and minPSI of <85%) and it was from highly expressed genes (average FPKM of >5.0 in at least one group), we classified it as a control alternative exon. As described previously, we examined the exon body, 250 bp of upstream and downstream introns, flanking exons, and 250-bp intronic regions of flanking exons to assign motif scores (33). Motif scores were assigned as the overall percentage of nucleotides covered by any of 12 ESRP motifs within a 50-bp sliding window. We slid the window by 1 bp in each region.

Microarray data accession number. The RNA-Seq data from this publication have been submitted to the NCBI Gene Expression Omnibus repository (http://www.ncbi.nlm.nih.gov/geo/) under the accession number GSE75492.

RESULTS

Comprehensive determination of changes in AS during EMT. In order to study the AS regulatory network during EMT more comprehensively, we adapted a previously described EMT model using the human H358 epithelial non-small cell lung cancer (NSCLC) cell line (17). We generated an H358 clone stably expressing a doxycycline (Dox)-inducible cDNA encoding a Zeb1-mCherry fusion protein (Fig. 1A). Over a 7-day time course following Dox treatment, we validated the gradual downregulation of the epithelial cell marker CDH1 (E-cadherin) and upregulation of the mesenchymal cell marker VIM (vimentin), confirming that the cells underwent progressive EMT throughout this time course (Fig. 1A and B). As expected, the expression levels of the ESRPs were also progressively downregulated during the time course (Fig. 1B and C). To study dynamic changes in splicing during EMT, we isolated total RNA on each day of the EMT time course following Dox treatment and in a no-Dox-treated control in biological triplicates (Fig. 1A). We performed strand-specific 100-bp paired-end RNA-Seq and obtained between 40 million and 70 million read pairs per replicate with a total of 1.3 billion read pairs. The use of biological replicates and high sequencing depth, together with the time course analysis, enabled the identification of a comprehensive program of AS switches associated with EMT. To fully characterize the AS program during the process of EMT, we used the rMATS computational pipeline to identify splicing changes, comparing each time point to no-Dox controls, and identified numerous cassette exons (also referred to as skipped exons [SEs]) that show significant splicing changes in at least one rMATS comparison (32). We applied a network analysis to identify clusters of SE events that had distinct temporal patterns of splicing changes across the EMT time course (Fig. 1D; see also Table S1 in the supplemental material). The two largest clusters consisted of SEs that showed either a graded increase (cluster 1) or a decrease (cluster 2) in splicing across the EMT time course. However, we also identified other clusters representing less straightforward temporal patterns of splicing changes at early or

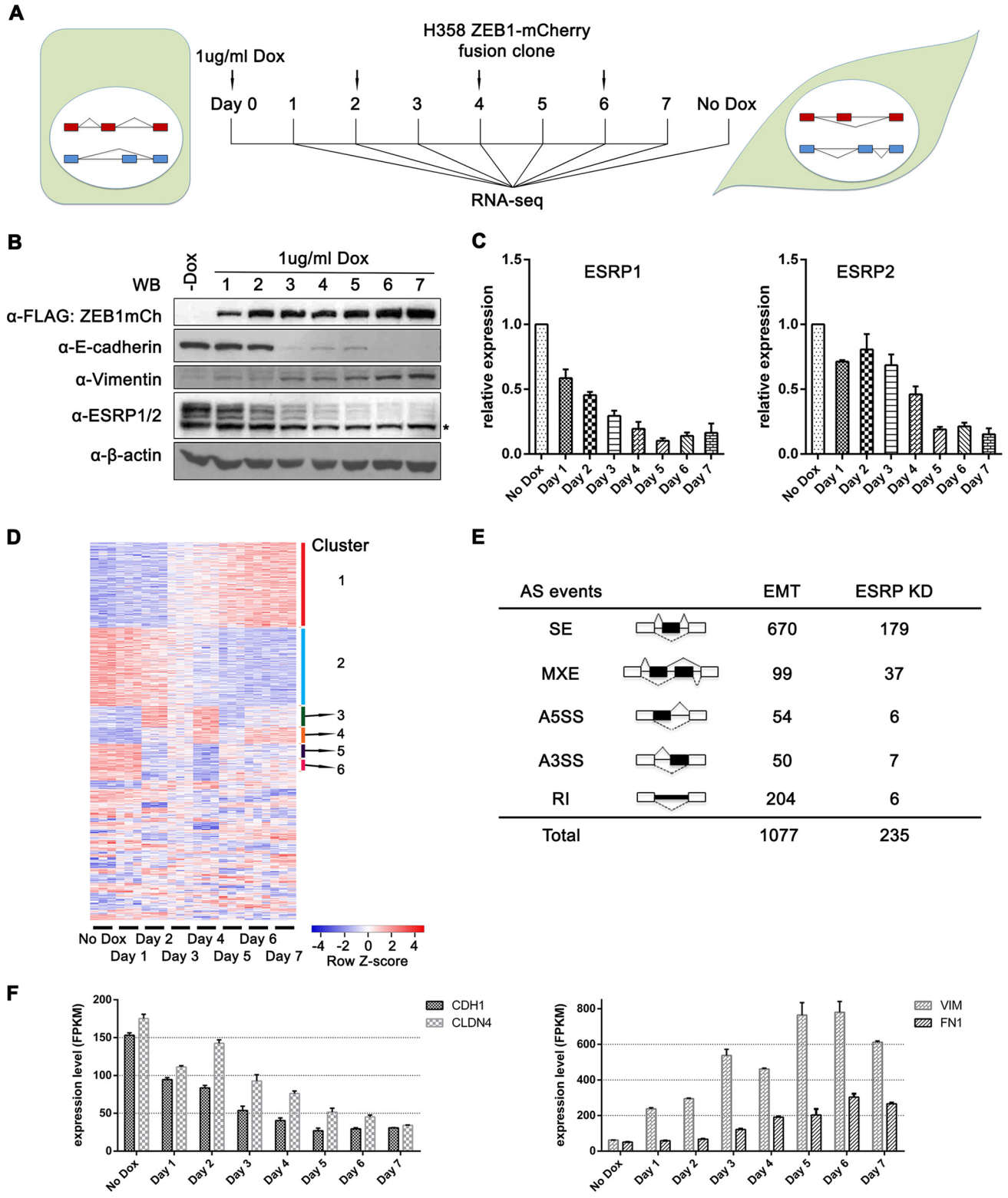

FIG 1 Comprehensive determination of changes in AS during EMT. (A) Schematic of the *in vitro* EMT model in human epithelial H358 cells. (B) Validation of Zeb1 induction upon Dox treatment and decreased expression of epithelial marker (E-cadherin [CDH1]), increased expression of mesenchymal marker (vimentin [VIM]), and decreased expression of ESRP1/2 during the time course by Western blotting (WB). β-Actin is used as a loading control. Multiple bands in the anti-ESRP1/2 blot represent different splice isoforms for ESRP1. The asterisk indicates a nonspecific cross-reacting band. (C) Quantitative RT-PCR (qRT-PCR) analysis of *ESRP1* and *ESRP2* showed decreased transcript levels during the time course (in biological triplicates). For all qRT-PCR analyses whose results are shown in this and subsequent figures, graphs show mean results and error bars represent standard deviations. (D) Heat map of the results for all identified SEs that significantly changed in splicing between time points, compared to controls, in at least one rMATS comparison, revealing two major clusters of SE events. Clusters with at least five SE events are shown (complete clusters and more details are shown in Table S1 in the supplemental material). (E) Summary of different types of significant AS events identified from comparison of day 7 and no-Dox cells and the ESRP1/2 knockdown (KD) experiment. SE, skipped exon; MXE, mutually exclusive exon; A5SS, alternative 5′ splice site; A3SS, alternative 3′ splice site; RI, retained intron. (F) RNA-Seq data (from biological triplicates) confirmed the downregulation of epithelial markers (*CDH1* and *CLND4*) and upregulation of mesenchymal markers (*VIM* and *FN1*) during the time course.

late time points, illustrating the complexity of temporally dynamic regulation of AS during EMT. We identified a total of 1,077 significant AS events (|ΔPSI| of >5% and FDR of <5%) at day 7 compared to the results for controls, the majority of which were cassette exons (670/1,077) (Fig. 1E; see also Table S1). Using gene expression profiling, we detected more than 2,000 genes with an expression change of at least twofold after 7 days of Dox treatment compared to their expression in controls (see Table S1). These included downregulation of epithelial markers *CDH1* and *CLDN4* and upregulation of mesenchymal markers *VIM* and *FN1* (fibronectin 1) (Fig. 1F). Consistent with the notion that genes under posttranscriptional regulation during cellular transitions are generally not regulated at the transcriptional level (37), only 74 target transcripts with splicing changes during EMT showed an expression change of at least twofold at the whole-transcript level. These findings reinforce the concept that transcription and AS are separate layers of gene expression regulation that are integrated during important developmental and physiological transitions.

ESRP1 and ESRP2 are major regulators of AS during EMT. Our previous studies showed that the ESRPs were important for the regulation of many AS events that switched in a different EMT model (19). However, the extent to which the ESRPs contribute to the AS regulatory network in EMT required further investigation. We therefore used lentiviral short hairpin RNAs (shRNAs) to deplete both ESRP1 and ESRP2 in H358 cells (Fig. 2A to C). We isolated total RNA from ESRP1/2 knockdown or control cells in biological triplicates and conducted strand-specific, 100-bp paired-end RNA-Seq with about 50 million read pairs per replicate and 320 million read pairs in total (Fig. 2A). Using the same rMATS pipeline, we identified 235 significant AS events (|ΔPSI| of >5% and FDR of <5%) regulated by the ESRPs, including 179 cassette exons, some of which were previously reported ESRP targets in other cell lines (Fig. 1E and 2D; see also Table S1 in the supplemental material) (19, 27, 30). Fewer than 50 genes showed an expression change of at least twofold upon ESRP1/2 knockdown (29 downregulated and 18 upregulated) (see Table S1). Gene ontology enrichment analysis using the DAVID functional annotation tool (https://david.ncifcrf.gov/home.jsp) showed that EMT-associated AS genes are involved in biological processes, such as RNA splicing, regulation of small GTPase-mediated signal transduction, and cytoskeleton organization, which are relevant to EMT (Fig. 2E) (38). The same analysis revealed that ESRP-regulated AS transcripts are enriched for genes involved in cell junction organization and cytoskeleton organization, consistent with our previous study (Fig. 2E) (19, 27).

To define the degree to which ESRP downregulation contributes to the global changes in AS during EMT, we analyzed the overlap between ESRP-regulated AS events and EMT-associated AS events (Fig. 3A; see also Table S2 in the supplemental material). The majority (68% [122/179]) of ESRP-regulated cassette exons also showed splicing changes during EMT, based on the rMATS analysis. As predicted, for all of these 122 events, the ESRPs promote the epithelial splicing patterns that are abrogated during EMT. Of the 670 cassette exons that showed splicing switches during EMT, 122 are regulated by the ESRPs, based on the rMATS analysis, which is highly significant ($P = 8.55E-117$). To validate these RNA-Seq results, we used semiquantitative RT-PCR for some representative cassette exons whose inclusion or exclusion was promoted by EMT or ESRP1/2 knockdown. Among seven tested ESRP-regulated, EMT-associated cassette exons predicted by rMATS, five were validated both in EMT and upon ESRP depletion (Fig. 3B). In the case of *CARD19*, the splicing change was validated in EMT and the same change was also observed after ESRP depletion, but the difference did not reach statistical significance. For *RPS24*, the splicing change was not validated in either setting. Importantly, knockdown of ESRP often induced splicing changes that were less than those observed during EMT (e.g., for *PLOD2*, *INF2*, and *NFYA*), despite similar levels of reduction for ESRP transcripts in both settings, indicating that ESRP depletion alone often cannot fully account for the degree of splicing changes we observed during EMT.

In addition to cassette exons with altered splicing during EMT, as well as with ESRP depletion according to the rMATS analysis, there were a significant number of EMT-associated AS events that were not identified as ESRP targets using the same statistical thresholds (88% [548/670]). However, we noted that many of those AS events in this analysis included exons previously shown to be ESRP targets in other systems or that were picked up in the rMATS analysis but were below the statistical cutoffs used to confidently identify ESRP-regulated targets (e.g., *MBNL1*, *ARHGEF11*, and *EXOC7*). Given the known limitations of RNA-Seq for detecting AS changes in less highly expressed genes and those with smaller delta PSI values, we suspect that the number of ESRP-regulated events was underestimated using the stringent criteria we applied. To further verify this, we selected 13 targets from a total of 51 AS events that showed at least 30% change of PSI during EMT while not being identified upon ESRP1/2 knockdown. For these events, we analyzed the splicing changes during EMT and upon ESRP1/2 knockdown (Fig. 3C). While four targets (*SPATS2L*, *IMPA1*, *WARS*, and *KIAA1468*) showed no significant splicing changes during EMT or ESRP1/2 knockdown, nine were validated as EMT-associated AS targets. However, seven of these nine validated EMT-associated cassette exons (77.8%) are also regulated by the ESRPs, albeit generally with a smaller change in splicing than during EMT. We also selected a subset of targets from the 57 significant splicing events that were identified upon ESRP1/2 knockdown but not during EMT based on the rMATS analysis. Among the six cassette exons tested, five were indeed regulated by the ESRPs, but of these, *CEACAM1* and *RNF231* also showed an apparent splicing change during EMT (Fig. 3D). In the case of *GRHL1* and *EPN3*, we noted dramatic downregulation in the total transcript level during EMT, which made identification of isoform ratios difficult after EMT. We therefore suspect that some other targets eluded detection due to reduced total transcript level during EMT. Furthermore, among the 50 genes in which these AS events occur, 17 had at least a 1.5-fold decrease in the total transcript level during the EMT. In the case of *GRHL1*, we also note that the skipped isoform results in a premature stop codon that renders the transcript sensitive to nonsense-mediated decay (NMD) that likely leads to underdetection of the degree of induced exon skipping. Nonetheless, the observation that some events switch during EMT or upon ESRP depletion but not under both conditions further indicates that contributions by other splicing factors are involved in EMT.

In the previous study of EMT-associated splicing changes, Shapiro et al. (21) implicated RBFOX2 and PTBP1 as regulators of EMT splicing switches along with the ESRPs. However, they noted a statistically greater overlap with ESRP-regulated targets identified using splicing-sensitive microarrays ($P = 9.27E-16$) than with RBFOX2- or PTBP1-regulated events defined in UV cross-

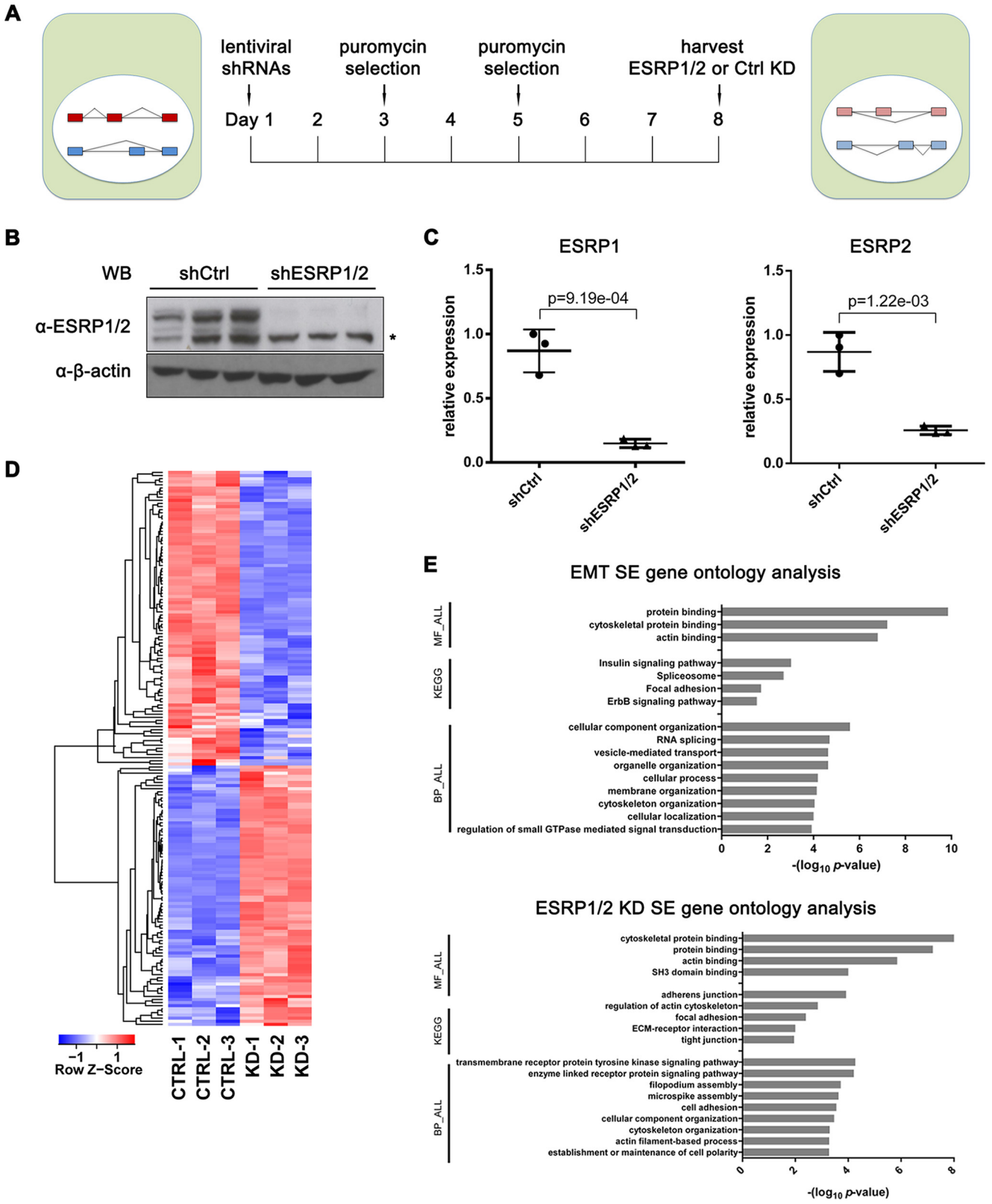

FIG 2 Identification of global changes in AS after ESRP1/2 depletion. (A) Schematic of ESRP1/2 knockdown experiment in H358 cells using lentiviral shRNAs. (B) Western blot validation of ESRP1/2 protein knockdown. (C) Validation of *ESRP1*/2 mRNA knockdown by qRT-PCR (from biological triplicates). A one-tailed unpaired *t* test was used to calculate the *P* value. The same statistical test was used in all subsequent qRT-PCR analyses whose results are shown in subsequent figures. (D) Heat map for ESRP-regulated skipped exons showed high consistency across replicates. (E) Gene ontology analysis for both EMT-associated and ESRP-regulated SE events showed an enrichment of EMT-relevant processes and pathways.

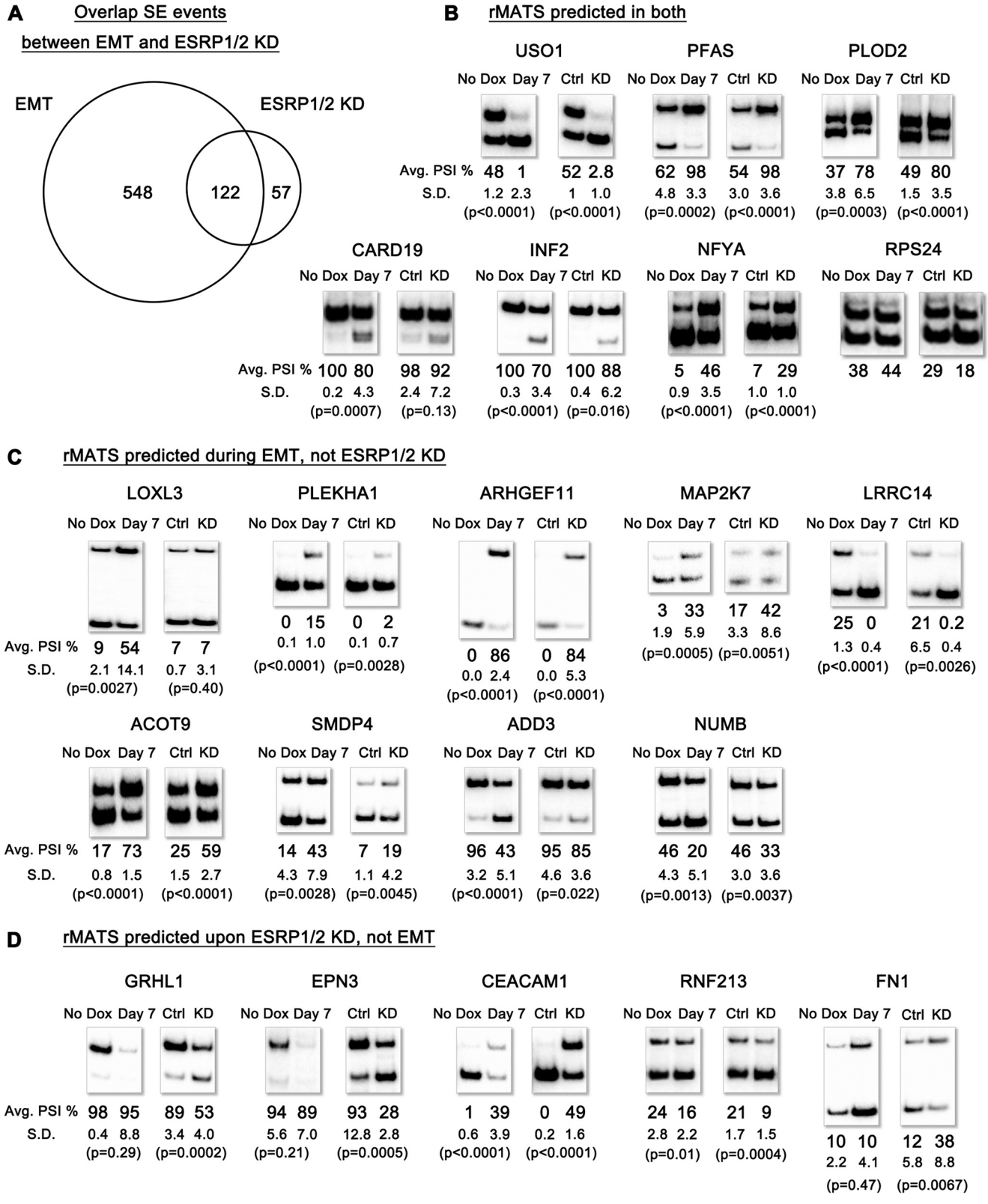

FIG 3 ESRP1 and ESRP2 are major regulators of AS during EMT. (A) Venn diagram of the overlap between EMT-associated cassette exons and those regulated upon ESRP1/2 knockdown based on rMATS analysis. (B) RT-PCR validation of exons predicted to switch during EMT and with ESRP1/2 knockdown. RPS24 is shown as an example of negative results. For all RT-PCR validations, a representative gel is shown for each target, together with the averaged PSI (Avg. PSI) and standard deviation (S.D.) calculated from biological triplicates. A one-tailed unpaired *t* test was used to calculate the *P* value for each comparison. The same statistical test was used in all subsequent RT-PCR analyses whose results are shown in subsequent figures. (C) RT-PCR validation of exons predicted to switch during EMT but not ESRP1/2 knockdown. (D) RT-PCR validation of exons predicted as ESRP-regulated events that were not identified during EMT.

linking and immunoprecipitation coupled with high-throughput sequencing (CLIP-Seq) studies ($P = 8.58E{-}5$ and $P = 0.0013$, respectively) (21). Furthermore, as previously noted, we determined an even higher degree of statistical significance for the overlap of ESRP targets and those from EMT in H358 cells. A recent study proposed that HNRNPM is also a key splicing factor involved in AS regulation during EMT (39). However, when we compared the 324 HNRNPM-regulated cassette exons identified by rMATS using published RNA-Seq data to EMT-associated ones identified here, we found fewer (38) shared events ($P = 1.50E{-}10$) (39). Taken together, these observations suggest that ESRP1 and ESRP2 are major regulators of AS during EMT. However, the fact that we see that some EMT-associated AS events are not significantly regulated by the ESRPs prompted us to pursue roles for additional splicing factors that contribute to AS programs during EMT.

The splicing factor RBM47 regulates splicing changes for a subset of AS events during EMT. To identify additional splicing factors that play a role in the regulation of AS during EMT, we first evaluated changes in expression for 446 RNA binding proteins after 7 days of Dox treatment compared to no-Dox controls, including all proteins that contain the most common canonical RNA binding domains, as well as additional proteins with known or putative roles in AS, such as those with arginine-serine (RS)–rich domains (Fig. 4A). We identified 48 RBPs with an expression change of at least 1.5-fold when comparing the results for day 7 to the expression in controls (averaged FPKM of >1 under at least one condition) (see Table S3 in the supplemental material). Among these, *ESRP1* and *ESRP2* show the largest changes in total expression, with a 10-fold decrease for *ESRP1*. Notably, we did not observe a substantial change in the *RBFOX2* expression level (less than 10% increase) in this EMT model. To further extend this analysis, we also carried out a cluster analysis for a subset of 166 RBPs (averaged FPKM of >5 under at least one condition) to identify temporal patterns of expression changes that might correspond to those observed in certain splicing clusters (Fig. 4B; see also Table S1). We noted that *ESRP1* and *ESRP2* were both in a cluster (cluster IV) that showed a graded decrease in total transcript level that was similar to the temporal patterns of splicing changes observed for the top two splicing clusters (clusters 1 and 2). These observations suggested that events in these two clusters are more likely to be regulated by the ESRPs. Consistent with this prediction, we noted that ESRP-regulated exons from rMATS analysis were statistically enriched in cluster 1 or 2 compared to a background set of EMT-associated SEs that were not in either cluster ($P = 4.95E{-}28$). The same cluster revealed a similar graded reduction in the expression of RBM47, which showed a 50% decrease in the total transcript level when comparing the results for day 7 to those for the no-Dox control and was confirmed by qRT-PCR, although only a modest change at the protein level was apparent using standard Western blot analysis (Fig. 4C). We therefore further investigated potential roles for RBM47 in the regulation of AS during EMT. RBM47 was recently shown to regulate pre-mRNA splicing and mRNA stability, as well as RNA editing (36, 40). Among a set of the published AS events that changed upon overexpression of RBM47 in MDA-MB-231-BrM2 cells, we noted several cassette exons that are either known ESRP targets or are among SE events that switch splicing during EMT (36). For example, both RBM47 and the ESRPs promote exclusion of the 36-nucleotide (nt) exon 7 in *MBNL1*, while both promote inclusion of the 81-nt exon 12 in *MAP3K7*. Notably, both alternatively spliced exons are EMT-associated AS events, suggesting potential combinatorial regulation during EMT.

To further investigate the role of RBM47 in enforcing epithelial splicing patterns that are altered during EMT, we depleted RBM47 in H358 cells with an shRNA and used RNA-Seq to determine the AS program regulated by RBM47 (Fig. 4D). Using the rMATS pipeline, we identified 117 significant AS events ($|\Delta PSI|$ of >5% and FDR of <5%), including 90 cassette exons (see Table S4 in the supplemental material). We evaluated the overlap of RBM47-regulated cassette exons with those that switch during EMT, as well as ESRP-regulated exons. We found 43 out of 90 RBM47-regulated cassette exons that were also predicted to change during EMT ($P = 1.37E{-}29$) (Fig. 4E; see also Table S4). However, although RBM47 promotes epithelial splicing patterns for most of these targets (27/43), it was also predicted to promote mesenchymal splicing patterns for 16 target transcripts. We validated a number of these RBM47-regulated targets, confirming that, indeed, downregulation of RBM47 likely contributes to some but not all splicing changes during EMT (Fig. 4F to H). We also validated all these RBM47-regulated AS events using an siRNA targeting a different region in the RBM47 transcript than was targeted by the shRNA used in the RNA-Seq experiment to confirm that these changes were due to RBM47 depletion (data not shown).

Among the 43 shared targets, 31 events (72.1%) are also regulated by the ESRPs based on the rMATS analysis, indicating a significant overlap of coregulated AS events for these regulators, the majority of which (19/31) are regulated in the same direction by the ESRPs and RBM47 (Fig. 4E). This complex combinatorial regulation between the ESRPs and RBM47 on AS is similar to that previously shown for the ESRPs and RBFOX2, where they usually but not always promote opposite changes in splicing, which is consistent with a function for RBFOX2 to usually but not always promote mesenchymal splicing patterns (27). To further investigate the combined roles of the ESRPs and RBM47 on their common targets, we tested the effect on AS following knockdown of ESRP1/2 or RBM47 alone and with combined knockdown of both regulators in H358 cells (Fig. 5A and B). For *MBNL1*, *CLSTN1*, *MACF1*, and *MAP3K7*, knockdown of ESRP1/2 or RBM47 alone induced a partial splicing switch toward the mesenchymal splicing pattern, whereas the combined knockdown revealed an additive switch in splicing, consistent with each contributing to the loss of epithelial cell-specific splicing during EMT (Fig. 5C). In contrast, for *TJP1*, *TCIRG1*, *ACSF2*, *MYO1B*, and *ITGA6*, the ESRPs and RBM47 were predicted to have different or opposite effects (Fig. 5D). While we did not observe a significant change in *TJP1* splicing with ESRP depletion, RBM47 knockdown induced a change in splicing opposite to that which occurred during EMT. For the other targets, ESRP1/2 knockdown induced a change in splicing consistent with that during EMT, which is opposite to that observed in RBM47 knockdown, indicating that the effect of ESRP downregulation during EMT predominated over that of RBM47. Based on these collective observations, we suspect that for exons where the ESRPs and RBM47 have opposing functions, the reduction in ESRP expression plays a more prominent role in the splicing switches that occur during EMT. Hence, whereas the downregulation of both the ESRPs and RBM47 together can account for the degree of some splicing switches observed during EMT, the effect of RBM47 to maintain epithelial splicing is less consistent

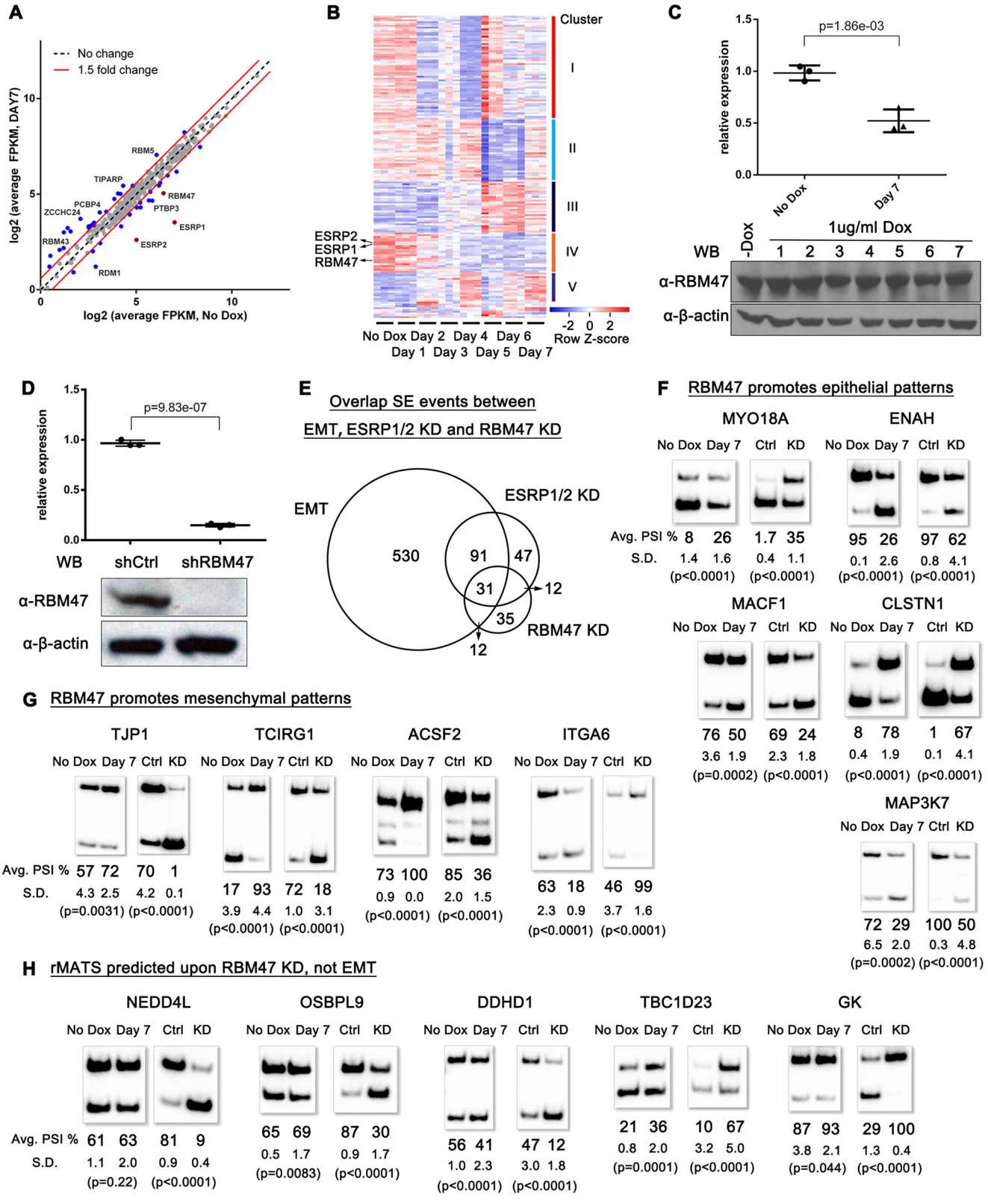

FIG 4 RBM47 regulates AS during EMT. (A) Candidate splicing factors that change expression during EMT; the subset that showed >1.5-fold change in expression level (FPKM of >1.0) is highlighted in blue or in red (*ESRP1*, *ESRP2*, and *RBM47*). (B) Heat map of cluster analysis revealed five major temporal patterns of expression changes for 166 RBPs (see Table S1 in the supplemental material for more details). (C) qRT-PCR validated a twofold decrease at the mRNA level for RBM47 at day 7 versus the no-Dox control during EMT, while Western blotting only showed a modest change at the protein level. (D) Knockdown of RBM47 in H358 cells using lentiviral shRNAs (in biological triplicate). (E) Venn diagram of the overlap between EMT-associated cassette exons and those regulated upon ESRP1/2 and RBM47 knockdown. (F) Validation of representative exons where RBM47 promotes epithelial splicing patterns. (G) Validation of representative exons where RBM47 promotes mesenchymal splicing patterns. For *ACSF2*, there is an alternative 5′ splice site at the end of the cassette exon, which yields the middle band in between the included/skipped PCR products. Only the top and bottom bands are quantified to calculate the PSI. (H) Validation of RBM47-regulated exons that were not predicted to switch during EMT.

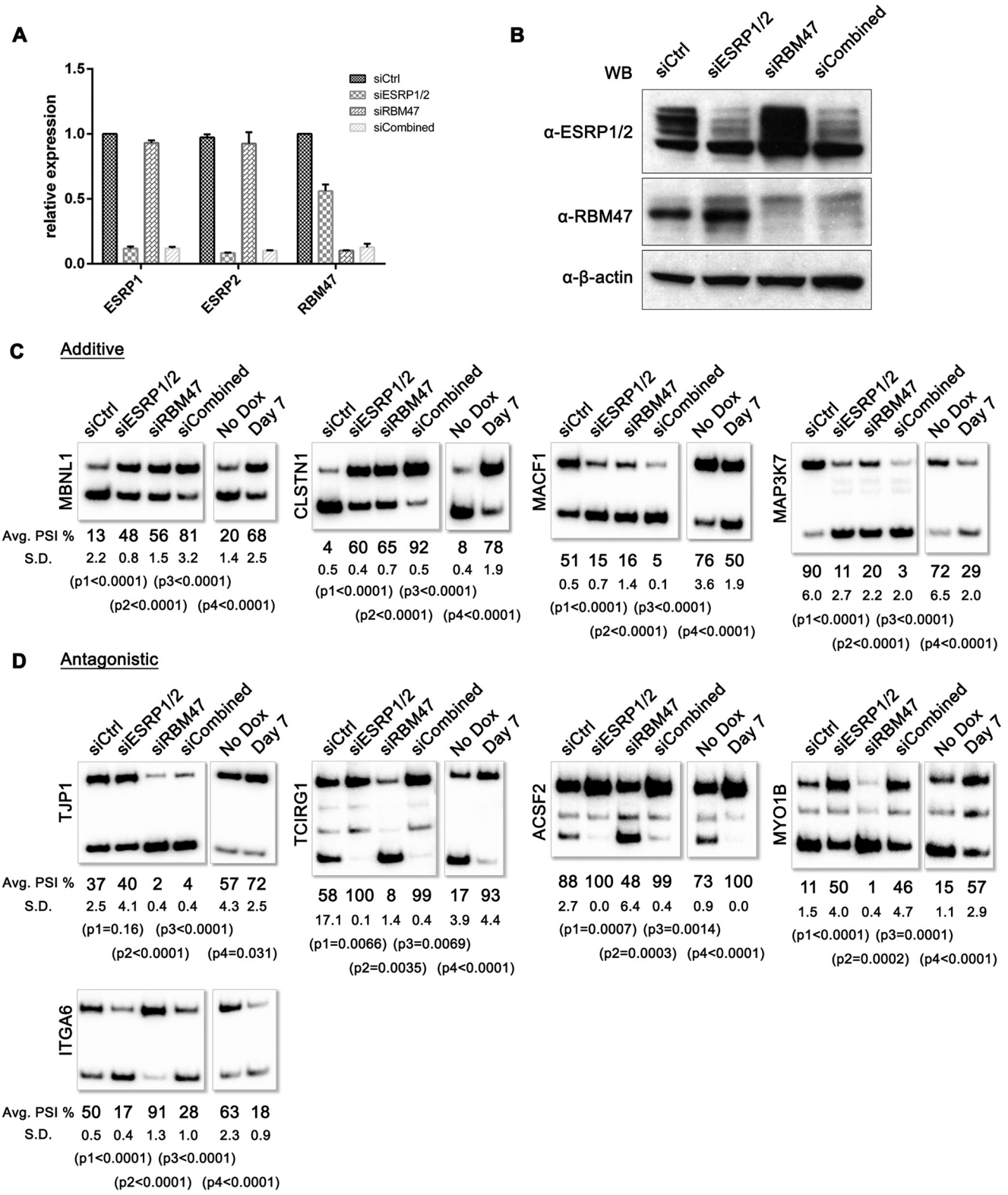

FIG 5 Combinatorial regulation of AS during EMT by ESRP1/2 and RBM47. (A) Validation by qRT-PCR of *ESRP1*, *ESRP2*, and *RBM47* mRNA depletion using siRNAs (in biological triplicates). (B) Western blot validation of knockdown of ESRP1/2 and RBM47 protein. Note that *RBM47* mRNA showed a 50% reduction upon ESRP1/2 knockdown, while the protein level did not change appreciably. (C) Validation of representative exons where ESRP1/2 and RBM47 knockdown have additive functions to promote splicing changes that occur during EMT. p1, p2, and p3 are *P* values comparing siESRP1/2, siRBM47, and siCombined to siCtrl, respectively, and p4 is to compare day 7 to no Dox. (D) Validation of representative exons where ESRP1/2 and RBM47 promote different or opposite changes in splicing. For *MYO1B*, there are two consecutive cassette exons (both are 87 nt in length) that can be included individually (middle band) or together in tandem (top band) or skipped together (bottom band). Only the top and bottom bands are quantified to calculate the PSI.

than that of the ESRPs. Although the mechanism underlying the complicated combinatorial regulation is largely unclear, these results further indicate that the EMT-associated AS network is fine-tuned by multiple regulators.

QKI promotes mesenchymal splicing patterns for AS events during EMT. We also considered contributions by splicing factors that did not demonstrate substantial changes in expression level during EMT. For example, the aforementioned RBFOX2 promotes predominantly mesenchymal splicing despite not showing a substantial change in total transcripts in our EMT model. Additionally, HNRNPM also did not change expression in our EMT model despite previous evidence that it promotes the mesenchymal splicing pattern for *CD44*, whereas we showed that the ESRPs promote the epithelial splicing pattern for *CD44* (30, 39). In this more recent study, it was similarly proposed that HNRNPM can only promote mesenchymal splicing patterns following abrogation of ESRP expression during EMT.

To uncover other EMT splicing regulators, including those without clear expression changes, we performed a motif enrichment analysis for 115 known splicing factor binding motifs flanking cassette exons that switch during EMT or ESRP1/2 knockdown (Fig. 6A and data not shown). In a previous study, we determined that the ESRPs bind to UGG-rich motifs *in vitro* by using systematic evolution of ligands by exponential enrichment coupled with high-throughput sequencing (SELEX-Seq) (27). These UGG-rich motifs are enriched in the vicinity of ERSP-regulated exons, consistent with an RNA map in which the ESRPs regulate splicing in a position-dependent manner: binding in the downstream intron promotes exon inclusion, while binding within or upstream from an exon promotes exon skipping. This RNA map is similar to those of the previously characterized splicing regulators NOVA and RBFOX2 (19, 41, 42). Accordingly, we confirmed the enrichment of ESRP1 binding sites downstream from ESRP-enhanced exons and upstream from ESRP-silenced exons in H358 cells (data not shown). RBFOX2 shows an opposite enrichment pattern flanking ESRP-regulated exons, further supporting the combinatorial but usually opposing functions of the ESRPs and RBFOX2 in AS regulation (data not shown). Consistent with the RNA maps for the ESRPs and RBFOX2, ESRP1 binding sites are enriched downstream from cassette exons that undergo skipping during EMT, whereas RBFOX2 binding sites are enriched downstream from cassette exons whose splicing increases during EMT (Fig. 6A and B). Similar to those of RBFOX2, QKI binding sites are enriched downstream from cassette exons, with increased inclusion following EMT (Fig. 6A). Previous reports showed that QKI also adheres to an RNA map in which binding in the downstream intron promotes exon inclusion, while binding in the upstream intron promotes skipping (43). Our motif analysis thus suggested a potential role for QKI in promoting inclusion of mesenchymal-specific exons.

QKI is an RNA binding protein belonging to the signal transduction and activation of RNA (STAR) family. It has been found to regulate multiple posttranscriptional processes, including pre-mRNA splicing, mRNA localization, mRNA stability, and protein translation (43–50). There are three major isoforms of QKI due to AS, QKI-5, QKI-6, and QKI-7 (51, 52). Among these, QKI-5 is predominantly nuclear, consistent with its function in regulating AS. In H358 cells, QKI-5 is the most abundant isoform, and we did not observe major isoform switches or significant expression changes during EMT (Fig. 6C). A recent study used RNA-Seq to characterize the AS events that change upon QKI knockdown in a lung cancer cell line (53). We noted that several of the QKI-regulated cassette exons identified in that study showed the opposite change in splicing from what we observed with ESRP depletion, suggesting opposing roles in splicing regulation during EMT. We therefore applied the rMATS pipeline that we used to define splicing switches during EMT, as well as ESRP1/2 and RBM47 knockdown, to the same data set and identified 70 QKI-regulated SE events. Compared to EMT-associated cassette exons, we found significant overlap with 35 shared target events despite the fact that they were identified in different cell lines ($P = 1.17E-24$) (see Table S5 in the supplemental material). Strikingly, for 33 of 35 QKI-regulated AS events associated with EMT, QKI promotes the mesenchymal splicing patterns, including 12 splicing events that are coregulated by the ESRPs. To further validate the RNA-Seq results, we knocked down QKI in the human mesenchymal breast cancer cell line MDA-MB-231 using two different siRNAs (siQKI 6 and 7) (Fig. 6D and E and data not shown). We tested 8 of the 33 AS events using semiquantitative RT-PCR. All 8 AS events were validated, and QKI indeed promoted the mesenchymal splicing patterns for all AS events tested, suggesting that QKI is a novel regulator of EMT-associated splicing switches that generally promotes mesenchymal splicing (Fig. 6F and data not shown).

DISCUSSION

We comprehensively determined an AS program associated with EMT in a Zeb1-inducible model. We showed that while the ESRPs are major splicing regulators for EMT, two other RBPs, namely, RBM47 and QKI, are also important for AS regulation during EMT. We further investigated the combinatorial regulation between the ESRPs and RBM47, by showing that they generally work cooperatively to promote epithelial splicing patterns, whereas QKI exclusively promotes mesenchymal splicing patterns. Based upon these findings we present a simplified model for combinatorial AS regulation during EMT involving the ESRPs, RBFOX2, QKI, and RBM47 (Fig. 7).

We showed that the ESRPs are the most downregulated RBPs in our H358 EMT model, which was also noted in a previous study using another EMT model (21). This observation suggested that the loss of ESRP1 and ESRP2 is most likely to contribute to more splicing switches during EMT than any other specific splicing factor or paralog family. Consistent with this proposal, based on previous results and the RNA-Seq analysis from our EMT model, the ESRPs were shown to have more significant overlap with EMT-associated splicing switches than other proposed EMT splicing factors, including RBFOX2, PTB, HNRNPM, RBM47, and QKI, although the use of different cell lines may affect the comparison. Notably, ESRP1/2 depletion in H358 cells didn't affect the protein level for RBM47 or QKI (data not shown). While many EMT-associated splicing switches were not identified as ESRP targets based on rMATS analysis, validation of a subset of such target transcripts revealed that the majority are in fact ESRP regulated, suggesting that many such events are at least partially regulated by the ESRPs, despite not passing our stringent statistical thresholds. However, whereas ESRP depletion induced splicing changes in the same direction as those observed during EMT, the change in PSI was frequently less than that during EMT despite a similar reduction in ESRP expression levels. In addition, motif

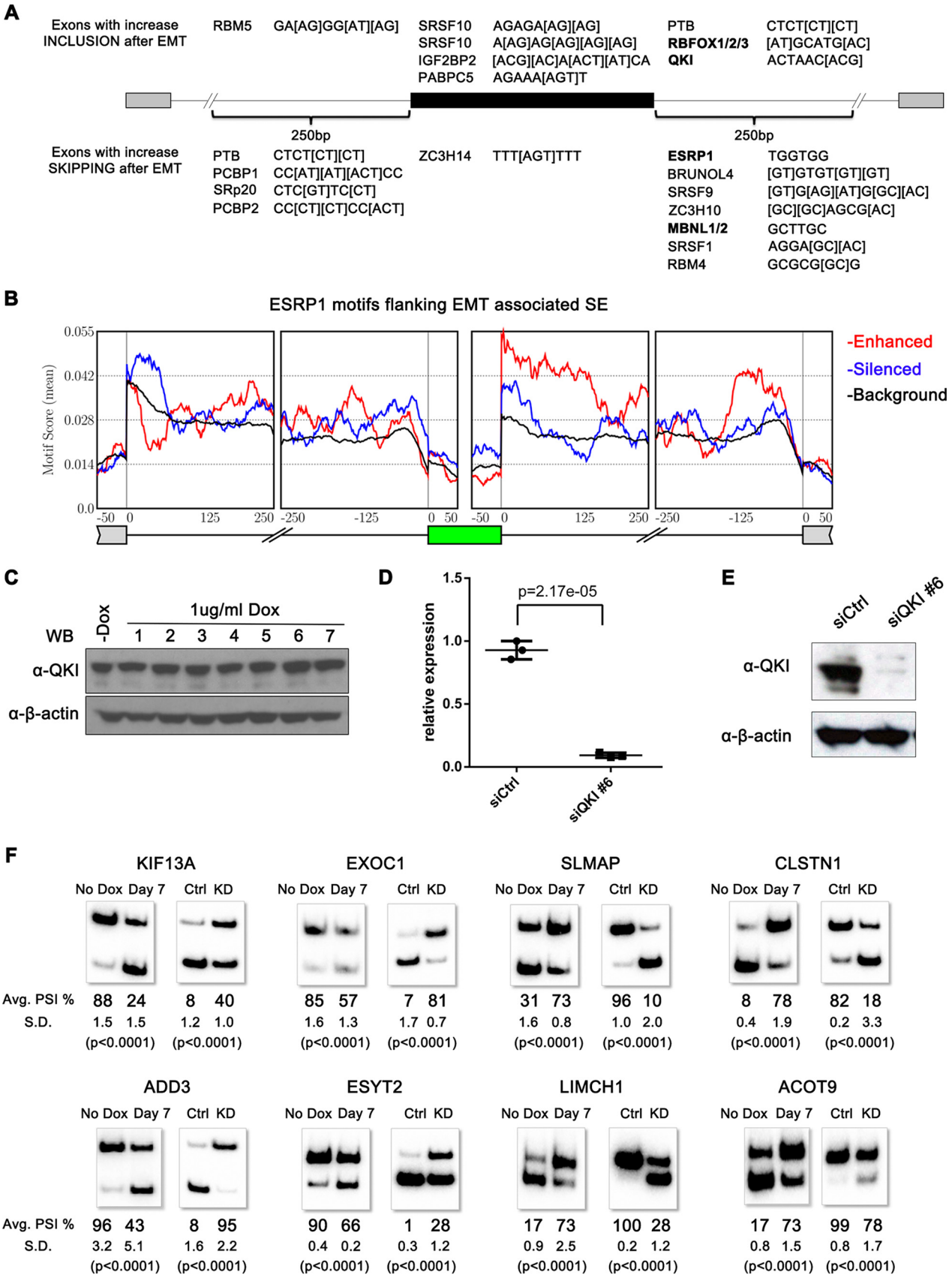

FIG 6 QKI promotes mesenchymal splicing patterns for AS events during EMT. (A) Known RBP motifs that are enriched flanking exons that switch splicing during EMT. (B) A map of ESRP1 binding motifs showing enrichment downstream from exons with increased skipping after EMT. (C) QKI protein level does not change detectably during EMT as determined by Western blotting. (D) Validation by qRT-PCR of *QKI* mRNA depletion in mesenchymal MDA-MB-231 cells using siRNA (biological triplicates). (E) Western blot validation of QKI protein knockdown. (F) Validation of representative exons where QKI promotes the mesenchymal splicing patterns upon knockdown with siQKI 6.

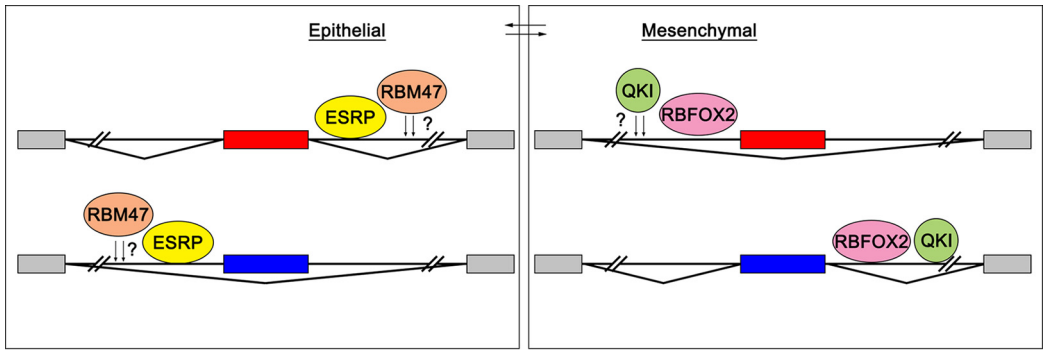

FIG 7 A model for AS regulation during EMT. In epithelial cells, the ESRPs bind to downstream introns and promote epithelial cell-specific exon inclusion, and they bind to upstream introns and promote exon skipping. While it is not clear whether RBM47 binds directly to some overlapping targets, it also helps to maintain epithelial splicing for a subset of exons. In mesenchymal cells, the expression levels of the ESRPs and RBM47 are decreased. In the absence of ESRP binding, RBFOX2 and QKI bind to downstream introns and promote mesenchymal cell-specific exon inclusion, while RBFOX2 also binds to upstream introns and promotes mesenchymal cell-specific exon skipping. QKI also can promote exon skipping, possibly also through binding in upstream introns.

analysis confirmed that ESRP1 binding sites are enriched downstream from cassette exons with decreased inclusion after EMT, supporting a direct role of the ESRPs in promoting inclusion of epithelial cell-specific exons. However, future studies using methods such as cross-linking immunoprecipitation followed by sequencing (CLIP-Seq) are needed to experimentally validate direct versus indirect targets.

We identified RBM47 as another splicing factor that is downregulated during EMT and showed that combined downregulation of the ESRPs and RBM47 can account for the complete EMT splicing change for at least some of these examples. This combinatorial regulation by the ESRPs and RBM47 usually promotes an additive effect on splicing, although there were some examples of opposing effects on splicing that indicate the complexity of combinatorial regulation of splicing during EMT. Motif analysis led to our discovery of QKI as also playing a role in the regulation of AS during EMT. QKI has been shown to bind to an ACUAAY motif both *in vitro* and *in vivo* and to either promote or inhibit splicing in a position-dependent manner (43, 54–56). Consistent with a direct function of QKI in promoting mesenchymal splicing, we found QKI binding motif enrichment downstream from cassette exons with increased inclusion after EMT. QKI showed a 40% increase in expression at the mRNA level but no appreciable change at the protein level during EMT, yet it promoted mesenchymal splicing for about 30 cassette exons. While we also did not observe splicing isoform changes in QKI during EMT, we cannot rule out the possibility that posttranslational modifications of QKI occur during EMT that alter its activity. Interestingly, a recent paper showed that QKI-5 promotes the formation of circular RNAs (circRNAs) that increase in abundance in EMT (57). It will be of interest to determine the degree to which QKI-regulated conventional AS events contribute to the EMT compared to AS events that generate circRNAs. Although we have shown that the ESRPs, RBM47, and QKI are responsible for a significant fraction of AS events during EMT, other splicing factors surely remain to be identified that also participate in combinatorial regulation of AS during this process.

A major challenge remains to define the functional consequences of AS switches that occur during EMT and how the changes in protein isoforms confer differential activities that affect the cellular changes that accompany this developmental transition. The complete functional dissection of any specific AS event requires detailed investigations at the molecular and cell biological level in order to characterize these differences. For example, an in-depth investigation into the AS of *EXOC7* (exocyst complex component 7) showed that the mesenchymal but not the epithelial isoform promotes actin polymerization and cell invasion in models of cancer metastasis (58). Another well-documented example is AS in *CD44* with a cluster of cassette exons in the pre-mRNA; while inclusion of one or more of these exons leads to *CD44* variant isoforms (*CD44v*, epithelial isoforms), exclusion of all cassette exons generates the *CD44* standard isoform that promotes EMT (*CD44s*, mesenchymal isoform). The transition from *CD44v* to *CD44s* was proposed to play a central role in EMT (59). In previous work, we also discussed several genes with known or predicted isoform-specific functions, such as *NUMB*, *EPB41L5*, and *TCF7L2*, that may contribute to processes that affect EMT (19, 27). While there are limited examples of other EMT-associated splicing switches that have been functionally well characterized, there are a number of transcripts identified here with functions that are relevant to EMT, such as epithelial cell adhesion and polarity. It therefore merits further investigation as to how the epithelial versus mesenchymal isoforms differentially affect these functions. For example, ADD3 (adducin 3), a subunit of the adducin family, is a membrane skeletal protein involved in the assembly of the spectrin-actin network at the membrane-cytoskeleton interface and is localized at cell-cell contacts of epithelial cells (60, 61). It was shown to colocalize with E-cadherin and CTNNB1 (or β-catenin) at AJs in epithelial cells, and knockdown of adducin significantly attenuated calcium-dependent AJ and TJ assembly and accelerated junctional disassembly, indicating that it is essential for the stability of epithelial junctions (62). ADD3 was also shown to be required for desmosomal cohesion in keratinocytes (63). It is notable that these roles are regulated by phosphorylation, as is the stability of the protein (64). The cassette exon in *ADD3*, whose inclusion decreased significantly after EMT, contains several known or predicted phosphorylation sites, suggesting the possibility that the different isoforms have differential functions due to the presence or absence of specific phosphorylation events (65, 66). Therefore, this AS event in *ADD3* during EMT

may affect functions of the protein in the maintenance of cell-cell junctions in epithelial cells that are relevant to EMT, but this requires further study.

Another potentially relevant example for which there have been some studies of isoform differences is *CEACAM1*, encoding or carcinoembryonic antigen-related cell adhesion molecule 1 (biliary glycoprotein), a member of the immunoglobulin superfamily specifically belonging to the carcinoembryonic antigen (CEA) family (67). The highly conserved 53-nt cassette exon residing in area encoding the C terminus, when included, generates a 71-amino-acid cytoplasmic tail (*CEACAM1* L isoform), while skipping of the exon generates a 9-amino-acid cytoplasmic tail (*CEACAM1* S isoform) (68). While both isoforms can mediate adhesive interaction, they have different adhesive properties, localizations, and posttranslational modifications on their unique cytoplasmic tails, suggesting distinct functions in mediating cell-cell interactions and signaling transduction for each isoform (69, 70). During EMT, there is a transition from primarily *CEACAM1* S isoform to about a 1:1 ratio of *CEACAM1* S and *CEACAM* L isoforms. Similarly, it was shown that normal breast epithelial cells predominantly express the *CEACAM1* S isoform, while the ratio of S/L isoforms is reduced in breast cancer cells (71). Since EMT is implicated in promoting tumorigenesis by changing cell-cell interactions and making individual cells more invasive, the antitumorigenesis property of CEACAM1 may partly rely on proper AS of *CEACAM1* (72).

In summary, our findings highlight the broad role of AS during EMT at a systems level and lay the groundwork for future studies focusing on specific AS events that have isoform-specific functions in EMT and related processes, such as metastasis, thus strengthening our understanding of development and tumorigenesis. The discovery of novel EMT splicing factors, namely, RBM47 and QKI, helps to extend our understanding of the AS regulatory network during EMT. The combinatorial regulation by the ESRPs and other splicing factors during EMT underscores how extensive interplays between different splicing factors affect dynamic changes in splicing during cellular transitions, as well as cell- and tissue-specific splicing.

ACKNOWLEDGMENTS

We thank Kimberly Dittmar, a former laboratory member, for reagents. We thank Ben Cieply for suggestions on the manuscript. We thank Kristen Lynch, Steve Liebhaber, Thomas Jongens, and Brian Gregory, as well as all the current laboratory members, for helpful discussions. We also thank Jonathan Schug and other personnel from Penn Genome Frontiers Institute (PGFI) and Next-Generation Sequencing Core (NGSC) facilities for consultation and RNA-Seq analysis.

We declare that we have no competing interests.

Y.Y. conducted all of the knockdown experiments for ESRP, RBM47, and QKI, participated in the RNA-Seq library preparation, carried out alternative splicing validations, and drafted the manuscript. J.W.P. processed the sequencing data and performed all of the rMATS analysis of alternative splicing, as well as motif and RNA map analysis. T.W.B. conducted EMT time course experiments and participated in the RNA-Seq library preparation. C.C.W. established stable Zeb1-inducible H358 cell lines and clones. Y.G. performed the network cluster analysis, with input from X.S. Y.X. designed and supervised all computational analyses. R.P.C. designed the study and drafted the manuscript. All authors read and approved the final manuscript.

FUNDING INFORMATION

This work, including the efforts of Xuequn Shang, was funded by Chinese National Natural Science Foundation (61332014). This work, including the efforts of Russ P. Carstens, was funded by HHS | NIH | National Institute of General Medical Sciences (NIGMS) (GM088809). This work, including the efforts of Yi Xing, was funded by HHS | NIH | National Institute of General Medical Sciences (NIGMS) (GM088342). This work, including the efforts of Russ P. Carstens, was funded by HHS | NIH | National Institute of Dental and Craniofacial Research (NIDCR) (DE024949). This work, including the efforts of Yang Guo, was funded by China Scholarship Council (CSC). This work, including the efforts of Yi Xing, was funded by Alfred P. Sloan Foundation. This work, including the efforts of Russ P. Carstens, was funded by HHS | NIH | National Institute of Arthritis and Musculoskeletal and Skin Diseases (NIAMS) (AR066741).

REFERENCES

1. **Pan Q, Shai O, Lee LJ, Frey BJ, Blencowe BJ.** 2008. Deep surveying of alternative splicing complexity in the human transcriptome by high-throughput sequencing. Nat Genet **40:**1413–1415. http://dx.doi.org/10.1038/ng.259.
2. **Wang ET, Sandberg R, Luo S, Khrebtukova I, Zhang L, Mayr C, Kingsmore SF, Schroth GP, Burge CB.** 2008. Alternative isoform regulation in human tissue transcriptomes. Nature **456:**470–476. http://dx.doi.org/10.1038/nature07509.
3. **Moroy T, Heyd F.** 2007. The impact of alternative splicing in vivo: mouse models show the way. RNA **13:**1155–1171. http://dx.doi.org/10.1261/rna.554607.
4. **Nilsen TW, Graveley BR.** 2010. Expansion of the eukaryotic proteome by alternative splicing. Nature **463:**457–463. http://dx.doi.org/10.1038/nature08909.
5. **Lee KY, Li M, Manchanda M, Batra R, Charizanis K, Mohan A, Warren SA, Chamberlain CM, Finn D, Hong H, Ashraf H, Kasahara H, Ranum LP, Swanson MS.** 2013. Compound loss of muscleblind-like function in myotonic dystrophy. EMBO Mol Med **5:**1887–1900. http://dx.doi.org/10.1002/emmm.201303275.
6. **Licatalosi DD, Yano M, Fak JJ, Mele A, Grabinski SE, Zhang C, Darnell RB.** 2012. Ptbp2 represses adult-specific splicing to regulate the generation of neuronal precursors in the embryonic brain. Genes Dev **26:**1626–1642. http://dx.doi.org/10.1101/gad.191338.112.
7. **Li Q, Zheng S, Han A, Lin C-H, Stoilov P, Fu X-D, Black DL.** 2014. The splicing regulator PTBP2 controls a program of embryonic splicing required for neuronal maturation. Elife **3:**e01201. http://dx.doi.org/10.7554/eLife.01201.
8. **Ule J, Jensen KB, Ruggiu M, Mele A, Ule A, Darnell RB.** 2003. CLIP identifies Nova-regulated RNA networks in the brain. Science **302:**1212–1215. http://dx.doi.org/10.1126/science.1090095.
9. **Gehman LT, Meera P, Stoilov P, Shiue L, O'Brien JE, Meisler MH, Ares M, Otis TS, Black DL.** 2012. The splicing regulator Rbfox2 is required for both cerebellar development and mature motor function. Genes Dev **26:**445–460. http://dx.doi.org/10.1101/gad.182477.111.
10. **Barash Y, Calarco JA, Gao W, Pan Q, Wang X, Shai O, Blencowe BJ, Frey BJ.** 2010. Deciphering the splicing code. Nature **465:**53–59. http://dx.doi.org/10.1038/nature09000.
11. **Lamouille S, Xu J, Derynck R.** 2014. Molecular mechanisms of epithelial-mesenchymal transition. Nat Rev Mol Cell Biol **15:**178–196. http://dx.doi.org/10.1038/nrm3758.
12. **Lim J, Thiery JP.** 2012. Epithelial-mesenchymal transitions: insights from development. Development **139:**3471–3486. http://dx.doi.org/10.1242/dev.071209.
13. **Nieto MA, Cano A.** 2012. The epithelial-mesenchymal transition under control: global programs to regulate epithelial plasticity. Semin Cancer Biol **22:**361–368. http://dx.doi.org/10.1016/j.semcancer.2012.05.003.
14. **Scheel C, Weinberg RA.** 2012. Cancer stem cells and epithelial-mesenchymal transition: concepts and molecular links. Semin Cancer Biol **22:**396–403. http://dx.doi.org/10.1016/j.semcancer.2012.04.001.
15. **Tiwari N, Gheldof A, Tatari M, Christofori G.** 2012. EMT as the ultimate survival mechanism of cancer cells. Semin Cancer Biol **22:**194–207. http://dx.doi.org/10.1016/j.semcancer.2012.02.013.
16. **Singh A, Settleman J.** 2010. EMT, cancer stem cells and drug resistance:

an emerging axis of evil in the war on cancer. Oncogene **29:**4741–4751. http://dx.doi.org/10.1038/onc.2010.215.
17. **Thomson S, Petti F, Sujka-Kwok I, Mercado P, Bean J, Monaghan M, Seymour SL, Argast GM, Epstein DM, Haley JD.** 2011. A systems view of epithelial-mesenchymal transition signaling states. Clin Exp Metastasis **28:**137–155. http://dx.doi.org/10.1007/s10585-010-9367-3.
18. **Taube JH, Herschkowitz JI, Komurov K, Zhou AY, Gupta S, Yang J, Hartwell K, Onder TT, Gupta PB, Evans KW, Hollier BG, Ram PT, Lander ES, Rosen JM, Weinberg RA, Mani SA.** 2010. Core epithelial-to-mesenchymal transition interactome gene-expression signature is associated with claudin-low and metaplastic breast cancer subtypes. Proc Natl Acad Sci U S A **107:**15449–15454. http://dx.doi.org/10.1073/pnas.1004900107.
19. **Warzecha CC, Jiang P, Amirikian K, Dittmar KA, Lu H, Shen S, Guo W, Xing Y, Carstens RP.** 2010. An ESRP-regulated splicing programme is abrogated during the epithelial-mesenchymal transition. EMBO J **29:**3286–3300. http://dx.doi.org/10.1038/emboj.2010.195.
20. **Warzecha CC, Shen S, Xing Y, Carstens RP.** 2009. The epithelial splicing factors ESRP1 and ESRP2 positively and negatively regulate diverse types of alternative splicing events. RNA Biol **6:**546–562. http://dx.doi.org/10.4161/rna.6.5.9606.
21. **Shapiro IM, Cheng AW, Flytzanis NC, Balsamo M, Condeelis JS, Oktay MH, Burge CB, Gertler FB.** 2011. An EMT-driven alternative splicing program occurs in human breast cancer and modulates cellular phenotype. PLoS Genet **7:**e1002218. http://dx.doi.org/10.1371/journal.pgen.1002218.
22. **Horiguchi K, Sakamoto K, Koinuma D, Semba K, Inoue A, Inoue S, Fujii H, Yamaguchi A, Miyazawa K, Miyazono K, Saitoh M.** 2012. TGF-beta drives epithelial-mesenchymal transition through deltaEF1-mediated downregulation of ESRP. Oncogene **31:**3190–3201. http://dx.doi.org/10.1038/onc.2011.493.
23. **Onder TT, Gupta PB, Mani SA, Yang J, Lander ES, Weinberg RA.** 2008. Loss of E-cadherin promotes metastasis via multiple downstream transcriptional pathways. Cancer Res **68:**3645–3654. http://dx.doi.org/10.1158/0008-5472.CAN-07-2938.
24. **Braeutigam C, Rago L, Rolke A, Waldmeier L, Christofori G, Winter J.** 2014. The RNA-binding protein Rbfox2: an essential regulator of EMT-driven alternative splicing and a mediator of cellular invasion. Oncogene **33:**1082–1092. http://dx.doi.org/10.1038/onc.2013.50.
25. **Venables JP, Brosseau J-P, Gadea G, Klinck R, Prinos P, Beaulieu J-F, Lapointe E, Durand M, Thibault P, Tremblay K, Rousset F, Tazi J, Abou Elela S, Chabot B.** 2013. RBFOX2 is an important regulator of mesenchymal tissue-specific splicing in both normal and cancer tissues. Mol Cell Biol **33:**396–405. http://dx.doi.org/10.1128/MCB.01174-12.
26. **Lapuk A, Marr H, Jakkula L, Pedro H, Bhattacharya S, Purdom E, Hu Z, Simpson K, Pachter L, Durinck S, Wang N, Parvin B, Fontenay G, Speed T, Garbe J, Stampfer M, Bayandorian H, Dorton S, Clark TA, Schweitzer A, Wyrobek A, Feiler H, Spellman P, Conboy J, Gray JW.** 2010. Exon-level microarray analyses identify alternative splicing programs in breast cancer. Mol Cancer Res **8:**961–974. http://dx.doi.org/10.1158/1541-7786.MCR-09-0528.
27. **Dittmar KA, Jiang P, Park JW, Amirikian K, Wan J, Shen S, Xing Y, Carstens RP.** 2012. Genome-wide determination of a broad ESRP-regulated posttranscriptional network by high-throughput sequencing. Mol Cell Biol **32:**1468–1482. http://dx.doi.org/10.1128/MCB.06536-11.
28. **Park SM, Gaur AB, Lengyel E, Peter ME.** 2008. The miR-200 family determines the epithelial phenotype of cancer cells by targeting the E-cadherin repressors ZEB1 and ZEB2. Genes Dev **22:**894–907. http://dx.doi.org/10.1101/gad.1640608.
29. **Gregory PA, Bert AG, Paterson EL, Barry SC, Tsykin A, Farshid G, Vadas MA, Khew-Goodall Y, Goodall GJ.** 2008. The miR-200 family and miR-205 regulate epithelial to mesenchymal transition by targeting ZEB1 and SIP1. Nat Cell Biol **10:**593–601. http://dx.doi.org/10.1038/ncb1722.
30. **Warzecha CC, Sato TK, Nabet B, Hogenesch JB, Carstens RP.** 2009. ESRP1 and ESRP2 are epithelial cell-type-specific regulators of FGFR2 splicing. Mol Cell **33:**591–601. http://dx.doi.org/10.1016/j.molcel.2009.01.025.
31. **Trapnell C, Williams BA, Pertea G, Mortazavi A, Kwan G, van Baren MJ, Salzberg SL, Wold BJ, Pachter L.** 2010. Transcript assembly and quantification by RNA-Seq reveals unannotated transcripts and isoform switching during cell differentiation. Nat Biotechnol **28:**511–515. http://dx.doi.org/10.1038/nbt.1621.
32. **Shen S, Park JW, Lu ZX, Lin L, Henry MD, Wu YN, Zhou Q, Xing Y.** 2014. rMATS: robust and flexible detection of differential alternative splicing from replicate RNA-Seq data. Proc Natl Acad Sci U S A **111:**E5593–E5601. http://dx.doi.org/10.1073/pnas.1419161111.
33. **Bebee TW, Park JW, Sheridan KI, Warzecha CC, Cieply BW, Rohacek AM, Xing Y, Carstens RP.** 2015. The splicing regulators Esrp1 and Esrp2 direct an epithelial splicing program essential for mammalian development. eLife **4:**e08954. http://dx.doi.org/10.7554/eLife.08954.
34. **Ray D, Kazan H, Cook KB, Weirauch MT, Najafabadi HS, Li X, Gueroussov S, Albu M, Zheng H, Yang A, Na H, Irimia M, Matzat LH, Dale RK, Smith SA, Yarosh CA, Kelly SM, Nabet B, Mecenas D, Li W, Laishram RS, Qiao M, Lipshitz HD, Piano F, Corbett AH, Carstens RP, Frey BJ, Anderson RA, Lynch KW, Penalva LO, Lei EP, Fraser AG, Blencowe BJ, Morris QD, Hughes TR.** 2013. A compendium of RNA-binding motifs for decoding gene regulation. Nature **499:**172–177. http://dx.doi.org/10.1038/nature12311.
35. **Anderson ES, Lin CH, Xiao X, Stoilov P, Burge CB, Black DL.** 2012. The cardiotonic steroid digitoxin regulates alternative splicing through depletion of the splicing factors SRSF3 and TRA2B. RNA **18:**1041–1049. http://dx.doi.org/10.1261/rna.032912.112.
36. **Vanharanta S, Marney CB, Shu W, Valiente M, Zou Y, Mele A, Darnell RB, Massague J.** 2014. Loss of the multifunctional RNA-binding protein RBM47 as a source of selectable metastatic traits in breast cancer. eLife **3:**e02734. http://dx.doi.org/10.7554/eLife.02734.
37. **Pan Q, Shai O, Misquitta C, Zhang W, Saltzman AL, Mohammad N, Babak T, Siu H, Hughes TR, Morris QD, Frey BJ, Blencowe BJ.** 2004. Revealing global regulatory features of mammalian alternative splicing using a quantitative microarray platform. Mol Cell **16:**929–941. http://dx.doi.org/10.1016/j.molcel.2004.12.004.
38. **Huang da W, Sherman BT, Lempicki RA.** 2009. Systematic and integrative analysis of large gene lists using DAVID bioinformatics resources. Nat Protoc **4:**44–57. http://dx.doi.org/10.1038/nprot.2008.211.
39. **Xu Y, Gao XD, Lee JH, Huang H, Tan H, Ahn J, Reinke LM, Peter ME, Feng Y, Gius D, Siziopikou KP, Peng J, Xiao X, Cheng C.** 2014. Cell type-restricted activity of hnRNPM promotes breast cancer metastasis via regulating alternative splicing. Genes Dev **28:**1191–1203. http://dx.doi.org/10.1101/gad.241968.114.
40. **Fossat N, Tourle K, Radziewic T, Barratt K, Liebhold D, Studdert JB, Power M, Jones V, Loebel DA, Tam PP.** 2014. C to U RNA editing mediated by APOBEC1 requires RNA-binding protein RBM47. EMBO Rep **15:**903–910. http://dx.doi.org/10.15252/embr.201438450.
41. **Licatalosi DD, Mele A, Fak JJ, Ule J, Kayikci M, Chi SW, Clark TA, Schweitzer AC, Blume JE, Wang X, Darnell JC, Darnell RB.** 2008. HITS-CLIP yields genome-wide insights into brain alternative RNA processing. Nature **456:**464–469. http://dx.doi.org/10.1038/nature07488.
42. **Zhang C, Zhang Z, Castle J, Sun S, Johnson J, Krainer AR, Zhang MQ.** 2008. Defining the regulatory network of the tissue-specific splicing factors Fox-1 and Fox-2. Genes Dev **22:**2550–2563. http://dx.doi.org/10.1101/gad.1703108.
43. **Hall MP, Nagel RJ, Fagg WS, Shiue L, Cline MS, Perriman RJ, Donohue JP, Ares M, Jr.** 2013. Quaking and PTB control overlapping splicing regulatory networks during muscle cell differentiation. RNA **19:**627–638. http://dx.doi.org/10.1261/rna.038422.113.
44. **Wu JI, Reed RB, Grabowski PJ, Artzt K.** 2002. Function of quaking in myelination: regulation of alternative splicing. Proc Natl Acad Sci U S A **99:**4233–4238. http://dx.doi.org/10.1073/pnas.072090399.
45. **Larocque D, Pilotte J, Chen T, Cloutier F, Massie B, Pedraza L, Couture R, Lasko P, Almazan G, Richard S.** 2002. Nuclear retention of MBP mRNAs in the quaking viable mice. Neuron **36:**815–829. http://dx.doi.org/10.1016/S0896-6273(02)01055-3.
46. **Li Z, Zhang Y, Li D, Feng Y.** 2000. Destabilization and mislocalization of myelin basic protein mRNAs in quaking dysmyelination lacking the QKI RNA-binding proteins. J Neurosci **20:**4944–4953.
47. **Chen AJ, Paik JH, Zhang H, Shukla SA, Mortensen R, Hu J, Ying H, Hu B, Hurt J, Farny N, Dong C, Xiao Y, Wang YA, Silver PA, Chin L, Vasudevan S, Depinho RA.** 2012. STAR RNA-binding protein Quaking suppresses cancer via stabilization of specific miRNA. Genes Dev **26:**1459–1472. http://dx.doi.org/10.1101/gad.189001.112.
48. **Zhao L, Mandler MD, Yi H, Feng Y.** 2010. Quaking I controls a unique cytoplasmic pathway that regulates alternative splicing of myelin-associated glycoprotein. Proc Natl Acad Sci U S A **107:**19061–19066. http://dx.doi.org/10.1073/pnas.1007487107.
49. **Saccomanno L, Loushin C, Jan E, Punkay E, Artzt K, Goodwin EB.**

1999. The STAR protein QKI-6 is a translational repressor. Proc Natl Acad Sci U S A **96:**12605–12610. http://dx.doi.org/10.1073/pnas.96.22.12605.
50. **Zhao L, Ku L, Chen Y, Xia M, LoPresti P, Feng Y.** 2006. QKI binds MAP1B mRNA and enhances MAP1B expression during oligodendrocyte development. Mol Biol Cell **17:**4179–4186. http://dx.doi.org/10.1091/mbc.E06-04-0355.
51. **Bockbrader K, Feng Y.** 2008. Essential function, sophisticated regulation and pathological impact of the selective RNA-binding protein QKI in CNS myelin development. Future Neurol **3:**655–668. http://dx.doi.org/10.2217/14796708.3.6.655.
52. **Ebersole TA, Chen Q, Justice MJ, Artzt K.** 1996. The quaking gene product necessary in embryogenesis and myelination combines features of RNA binding and signal transduction proteins. Nat Genet **12:**260–265. http://dx.doi.org/10.1038/ng0396-260.
53. **Zong FY, Fu X, Wei WJ, Luo YG, Heiner M, Cao LJ, Fang Z, Fang R, Lu D, Ji H, Hui J.** 2014. The RNA-binding protein QKI suppresses cancer-associated aberrant splicing. PLoS Genet **10:**e1004289. http://dx.doi.org/10.1371/journal.pgen.1004289.
54. **Galarneau A, Richard S.** 2005. Target RNA motif and target mRNAs of the Quaking STAR protein. Nat Struct Mol Biol **12:**691–698. http://dx.doi.org/10.1038/nsmb963.
55. **Hafner M, Landthaler M, Burger L, Khorshid M, Hausser J, Berninger P, Rothballer A, Ascano M, Jr, Jungkamp AC, Munschauer M, Ulrich A, Wardle GS, Dewell S, Zavolan M, Tuschl T.** 2010. Transcriptome-wide identification of RNA-binding protein and microRNA target sites by PAR-CLIP. Cell **141:**129–141. http://dx.doi.org/10.1016/j.cell.2010.03.009.
56. **Ryder SP, Williamson JR.** 2004. Specificity of the STAR/GSG domain protein Qk1: implications for the regulation of myelination. RNA **10:**1449–1458. http://dx.doi.org/10.1261/rna.7780504.
57. **Conn SJ, Pillman KA, Toubia J, Conn VM, Salmanidis M, Phillips CA, Roslan S, Schreiber AW, Gregory PA, Goodall GJ.** 2015. The RNA binding protein quaking regulates formation of circRNAs. Cell **160:**1125–1134. http://dx.doi.org/10.1016/j.cell.2015.02.014.
58. **Lu HZ, Liu JL, Liu SJ, Zeng JW, Ding DQ, Carstens RP, Cong YS, Xu XW, Guo W.** 2013. Exo70 isoform switching upon epithelial-mesenchymal transition mediates cancer cell invasion. Dev Cell **27:**560–573. http://dx.doi.org/10.1016/j.devcel.2013.10.020.
59. **Brown RL, Reinke LM, Damerow MS, Perez D, Chodosh LA, Yang J, Cheng CH.** 2011. CD44 splice isoform switching in human and mouse epithelium is essential for epithelial-mesenchymal transition and breast cancer progression. J Clin Invest **121:**1064–1074. http://dx.doi.org/10.1172/JCI44540.
60. **Gardner K, Bennett V.** 1987. Modulation of spectrin-actin assembly by erythrocyte adducin. Nature **328:**359–362. http://dx.doi.org/10.1038/328359a0.
61. **Kaiser HW, O'Keefe E, Bennett V.** 1989. Adducin: Ca++-dependent association with sites of cell-cell contact. J Cell Biol **109:**557–569. http://dx.doi.org/10.1083/jcb.109.2.557.
62. **Naydenov NG, Ivanov AI.** 2010. Adducins regulate remodeling of apical junctions in human epithelial cells. Mol Biol Cell **21:**3506–3517. http://dx.doi.org/10.1091/mbc.E10-03-0259.
63. **Rotzer V, Breit A, Waschke J, Spindler V.** 2014. Adducin is required for desmosomal cohesion in keratinocytes. J Biol Chem **289:**14925–14940. http://dx.doi.org/10.1074/jbc.M113.527127.
64. **Matsuoka Y, Li X, Bennett V.** 1998. Adducin is an in vivo substrate for protein kinase C: phosphorylation in the MARCKS-related domain inhibits its activity in promoting spectrin-actin complexes and occurs in many cells, including dendritic spines of neurons. J Cell Biol **142:**485–497. http://dx.doi.org/10.1083/jcb.142.2.485.
65. **Huttlin EL, Jedrychowski MP, Elias JE, Goswami T, Rad R, Beausoleil SA, Villén J, Haas W, Sowa ME, Gygi SP.** 2010. A tissue-specific atlas of mouse protein phosphorylation and expression. Cell **143:**1174–1189. http://dx.doi.org/10.1016/j.cell.2010.12.001.
66. **Lundby A, Secher A, Lage K, Nordsborg NB, Dmytriyev A, Lundby C, Olsen JV.** 2012. Quantitative maps of protein phosphorylation sites across 14 different rat organs and tissues. Nat Commun **3:**876. http://dx.doi.org/10.1038/ncomms1871.
67. **Barnett TR, Kretschmer A, Austen DA, Goebel SJ, Hart JT, Elting JJ, Kamarck ME.** 1989. Carcinoembryonic antigens—alternative splicing accounts for the multiple messenger-RNAs that code for novel members of the carcinoembryonic antigen family. J Cell Biol **108:**267–276. http://dx.doi.org/10.1083/jcb.108.2.267.
68. **Dráberová L, Černá H, Brodská H, Boubelík M, Watt SM, Stanners CP, Dráber P.** 2000. Soluble isoforms of CEACAM1 containing the A2 domain: increased serum levels in patients with obstructive jaundice and differences in 3-fucosyl-N-acetyl-lactosamine moiety. Immunology **101:**279–287. http://dx.doi.org/10.1046/j.1365-2567.2000.00113.x.
69. **Sundberg U, Obrink B.** 2002. CEACAM1 isoforms with different cytoplasmic domains show different localization, organization and adhesive properties in polarized epithelial cells. J Cell Sci **115**(Pt 6)**:**1273–1284.
70. **Huber M, Izzi L, Grondin P, Houde C, Kunath T, Veillette A, Beauchemin N.** 1999. The carboxyl-terminal region of biliary glycoprotein controls its tyrosine phosphorylation and association with protein-tyrosine phosphatases SHP-1 and SHP-2 in epithelial cells. J Biol Chem **274:**335–344. http://dx.doi.org/10.1074/jbc.274.1.335.
71. **Gaur S, Shively J, Yen Y, Gaur R.** 2008. Altered splicing of CEACAM1 in breast cancer: identification of regulatory sequences that control splicing of CEACAM1 into long or short cytoplasmic domain isoforms. Mol Cancer **7:**46. http://dx.doi.org/10.1186/1476-4598-7-46.
72. **Yang J, Weinberg RA.** 2008. Epithelial-mesenchymal transition: at the crossroads of development and tumor metastasis. Dev Cell **14:**818–829. http://dx.doi.org/10.1016/j.devcel.2008.05.009.